

# Tadpole renormalization and relativistic corrections in lattice NRQCD

Norman H. Shakespeare\* and Howard D. Trottier†

*Department of Physics, Simon Fraser University, Burnaby, B.C., Canada V5A 1S6*  
(February 1998)

## Abstract

We make a detailed comparison of two tadpole renormalization schemes in the context of the quarkonium hyperfine splittings in lattice NRQCD. We renormalize improved gauge-field and NRQCD actions using the mean-link  $u_{0,L}$  in Landau gauge, and using the fourth root of the average plaquette  $u_{0,P}$ . Simulations are done for the three quarkonium systems  $c\bar{c}$ ,  $b\bar{c}$ , and  $b\bar{b}$ . The hyperfine splittings are computed both at leading ( $O(M_Q v^4)$ ) and at next-to-leading ( $O(M_Q v^6)$ ) order in the relativistic expansion, where  $M_Q$  is the renormalized quark mass, and  $v^2$  is the mean-squared velocity. Results are obtained at a large number of lattice spacings, in the range of about 0.14 fm to 0.38 fm. A number of features emerge, all of which favor tadpole renormalization using  $u_{0,L}$ . This includes much better scaling behavior of the hyperfine splittings in the three quarkonium systems when  $u_{0,L}$  is used. We also find that relativistic corrections to the spin splittings are smaller when  $u_{0,L}$  is used, particularly for the  $c\bar{c}$  and  $b\bar{c}$  systems. We also see signs of a breakdown in the NRQCD expansion when the bare quark mass falls below about one in lattice units. Simulations with  $u_{0,L}$  also appear to be better behaved in this context: the bare quark masses turn out to be larger when  $u_{0,L}$  is used, compared to when  $u_{0,P}$  is used on lattices with comparable spacings. These results also demonstrate the need to go beyond tree-level tadpole improvement for precision simulations.

Typeset using REVTeX

---

\*Email address: nshakesp@sfu.ca.

†Email address: trottier@sfu.ca.

## I. INTRODUCTION

Tadpole improvement of lattice actions [1] has become an essential ingredient in numerical simulations of hadronic systems. Tadpole improvement has revitalized interest in simulations on coarse lattices, and is playing an important role in current efforts to extract continuum results from simulations on fine lattices.

Tadpole diagrams in lattice theories are induced by the nonlinear connection between the lattice link variables  $U_\mu$  and the continuum gauge fields. This has been shown to cause large radiative corrections to many quantities in lattice theories. Fortunately, most of the effects of tadpoles can be removed by a simple mean field renormalization of the links [1]

$$U_\mu(x) \rightarrow \frac{U_\mu(x)}{u_0}, \quad (1)$$

where an operator dominated by short-distance fluctuations is used to determine  $u_0$ .

One of the earliest applications of tadpole improvement was in the development of lattice nonrelativistic quantum chromodynamics (NRQCD) [2–7]. Precision simulations of the  $\Upsilon$  system in NRQCD have provided many important phenomenological results, including the strong coupling constant [4] and the  $b$ -quark pole mass [5,6]. However the situation for charmonium is more problematic, due to large relativistic corrections in this system [8].

In fact the quarkonium spectrum provides a powerful probe of tadpole renormalization. The quarkonium fine and hyperfine spin splittings in particular are very sensitive to the details of the NRQCD Hamiltonian, with the relevant operators undergoing large tadpole renormalizations. For example, it has been shown [8] that scaling of the charmonium hyperfine splitting is significantly improved when the tadpole renormalization is determined using the mean-link  $u_{0,L}$  measured in Landau gauge [1]:

$$u_{0,L} \equiv \left\langle \frac{1}{3} \text{ReTr} U_\mu \right\rangle, \quad \partial_\mu A_\mu = 0, \quad (2)$$

compared to when the fourth root of the average plaquette  $u_{0,P}$  is used:

$$u_{0,P} \equiv \left\langle \frac{1}{3} \text{ReTr} U_{\text{pl}} \right\rangle^{1/4}. \quad (3)$$

Equation (3) has been employed in most previous lattice simulations. First evidence for a more continuum-like behavior of lattice actions using  $u_{0,L}$  came from studies of rotational symmetry restoration in the heavy quark potential [9]. More recently, improved scaling of the charmonium spectrum from relativistic actions [10], and of the SU(2) glueball spectrum [11], have also been observed in simulations using  $u_{0,L}$ .

In this paper we make a detailed comparison of the two tadpole renormalization schemes  $u_{0,L}$  and  $u_{0,P}$  (when implemented at tree-level) in the context of the quarkonium hyperfine splittings in NRQCD. This is done for the three quarkonium systems  $c\bar{c}$ ,  $b\bar{c}$ , and  $b\bar{b}$ . The hyperfine splittings are computed both at leading ( $O(M_Q v^4)$ ) and at next-to-leading ( $O(M_Q v^6)$ ) order in the relativistic expansion, where  $M_Q$  is the renormalized quark mass, and  $v^2$  is the mean-squared velocity. Results are obtained at a large number of lattice spacings, in the range of about 0.14 fm to 0.38 fm. All quantities are calculated in the two tadpole schemes after careful re-tuning of the lattice action parameters for each system.

We find that scaling of the hyperfine splittings in all three quarkonium systems is significantly improved when  $u_{0,L}$  is used. This confirms and extends the scaling analysis done in Ref. [8]. In addition we see signs of a possible breakdown of the NRQCD effective action at smaller lattice spacings, when the bare quark mass in lattice units  $aM_Q^0$  falls below about one (scaling studies of the  $\Upsilon$  spectrum, as a probe of the NRQCD expansion, have previously been reported in Ref. [12]). Large changes in the  $c\bar{c}$  and  $b\bar{c}$  splittings with  $u_{0,P}$  are evident at smaller lattices spacings. Once again, simulations with  $u_{0,L}$  are better behaved in this context: the bare charm-quark mass turns out to be much larger when  $u_{0,L}$  is used, compared to when  $u_{0,P}$  is used on lattices with comparable spacings. Although there are clear pathologies in the  $u_{0,P}$  data at small bare masses, our conclusions here are necessarily tentative, since we are unable to do realistic simulations on sufficiently fine lattices to get  $aM_c^0$  appreciably below one with  $u_{0,L}$  tadpole improvement.

We also find that the choice of tadpole renormalization scheme has a strong effect on the apparent convergence of the velocity expansion which underlies the NRQCD effective action. We find that the relativistic corrections to the hyperfine splittings are smaller when  $u_{0,L}$  is used, particularly for the  $c\bar{c}$  and  $b\bar{c}$  systems. This casts new light on the results obtained in Ref. [8], where relativistic corrections to spin splittings in NRQCD were first calculated. The results obtained here using  $u_{0,L}$  to renormalize the action suggest that  $v_{c\bar{c}}^2 \approx 0.3$ , which is consistent with naive estimates of operator expectation values in NRQCD [3]. Hence while the velocity expansion for charmonium is subject to large corrections, it may not be as unreliable as was suggested in Ref. [8], where simulations with  $u_{0,P}$  on relatively fine lattices found  $v_{c\bar{c}}^2 \approx 0.6$ . (Relativistic corrections have more recently been analyzed in the  $\Upsilon$  system [13,14], and have also been studied in heavy-light mesons [15–17]).

Although these results clearly favor using  $u_{0,L}$  for tadpole improvement, they also serve to underline the need to go beyond tree-level matching of lattice actions. Results from this study and others (see e.g. Refs. [9–12]) demonstrate that precision results can only be obtained once uncertainties due to  $O(\alpha_s)$  renormalizations are removed (for some recent work in this connection see e.g. Refs. [18,19]).

## II. DETAILS OF THE SIMULATIONS

### A. Lattice Actions

The lattice NRQCD effective action for quarkonium is organized according to an expansion in the mean squared velocity  $v^2$  of the heavy quarks, with corrections included for lattice artifacts. The effective action, including spin-independent operators to  $O(v^4)$ , and spin-dependent interactions to  $O(v^6)$ , was derived in Ref. [3]. Following Refs. [6,7], we use the evolution equation

$$G_{t+1} = \left(1 - \frac{aH_0}{2n}\right)^n U_4^\dagger \left(1 - \frac{aH_0}{2n}\right)^n (1 - a\delta H) G_t \quad (t > 1), \quad (4)$$

where the initial evolution is set by

$$G_1 = \left(1 - \frac{aH_0}{2n}\right)^n U_4^\dagger \left(1 - \frac{aH_0}{2n}\right)^n \delta_{\vec{x},0}. \quad (5)$$

On the lattice the leading kinetic energy operator  $H_0$  is given by

$$H_0 = -\frac{\Delta^{(2)}}{2M_Q^0}, \quad (6)$$

where  $M_Q^0$  is the bare quark mass and  $\Delta^{(2)}$  is the lattice Laplacian.

Relativistic corrections are organized in powers of the heavy quark velocity:

$$\delta H = \delta H^{(4)} + \delta H^{(6)}. \quad (7)$$

$\delta H^{(4)}$  contains spin-independent relativistic corrections and leading-order spin interactions:

$$\begin{aligned} \delta H^{(4)} = & -c_1 \frac{(\Delta^{(2)})^2}{8(M_Q^0)^3} + c_2 \frac{ig}{8(M_Q^0)^2} (\tilde{\Delta} \cdot \tilde{\mathbf{E}} - \tilde{\mathbf{E}} \cdot \tilde{\Delta}) \\ & -c_3 \frac{g}{8(M_Q^0)^2} \boldsymbol{\sigma} \cdot (\tilde{\Delta} \times \tilde{\mathbf{E}} - \tilde{\mathbf{E}} \times \tilde{\Delta}) - c_4 \frac{g}{2M_Q^0} \boldsymbol{\sigma} \cdot \tilde{\mathbf{B}} \\ & + c_5 \frac{a^2 \Delta^{(4)}}{24M_Q^0} - c_6 \frac{a(\Delta^{(2)})^2}{16n(M_Q^0)^2}, \end{aligned} \quad (8)$$

with the last two terms coming from finite lattice spacing corrections to the lattice Laplacian and the lattice time derivative respectively. The parameter  $n$  is introduced to remove instabilities in the heavy quark propagator caused by high momentum modes [3]. Spin-dependent relativistic corrections for quarkonium first appear at  $O(v^6)$ :

$$\begin{aligned} \delta H^{(6)} = & -c_7 \frac{g}{8(M_Q^0)^3} \{ \tilde{\Delta}^{(2)}, \boldsymbol{\sigma} \cdot \tilde{\mathbf{B}} \}, \\ & -c_8 \frac{3g}{64(M_Q^0)^4} \{ \tilde{\Delta}^{(2)}, \boldsymbol{\sigma} \cdot (\tilde{\Delta} \times \tilde{\mathbf{E}} - \tilde{\mathbf{E}} \times \tilde{\Delta}) \}, \\ & -c_9 \frac{ig^2}{8(M_Q^0)^3} \boldsymbol{\sigma} \cdot \tilde{\mathbf{E}} \times \tilde{\mathbf{E}}. \end{aligned} \quad (9)$$

Spin-independent corrections at  $O(v^6)$  are not considered here (these operators may in fact have indirect effects on spin splittings [7,17]). As in Ref. [8] simulations were done with the derivative operators and the clover fields corrected for their leading discretization errors. This is indicated by the tilda superscripts on these operators in Eqs. (8) and (9). Complete expressions for the operators can be found in Refs. [3,8].

At tree-level all of the coefficients  $c_i$  in Eqs. (8) and (9) are one. However tadpole improvement is crucial in order to eliminate large radiative corrections. Independent sets of simulations were done using the two tadpole renormalization schemes described in Section I: the mean-link in Landau gauge, Eq. (2) (using a standard lattice implementation of the continuum Landau gauge fixing [20]), and the fourth root of the average plaquette, Eq. (3). The links were rescaled in the simulation before they were input to the quark propagator subroutine, to be sure that Eq. (1) was correctly implemented in all terms in the heavy quark action. The gauge-field configurations were generated using an  $O(a^4)$ -accurate tadpole-improved action [21]

$$S[U] = \beta \sum_{\text{pl}} \frac{1}{3} \text{ReTr} (1 - U_{\text{pl}}) - \frac{\beta}{20u_0^2} \sum_{\text{rt}} \frac{1}{3} \text{ReTr} (1 - U_{\text{rt}}), \quad (10)$$

where the sums are over all oriented  $1 \times 1$  plaquettes (pl) and  $1 \times 2$  rectangles (rt).

Meson creation operators were constructed from quark ( $\psi^\dagger$ ) and antiquark ( $\chi^\dagger$ ) creation operators [2,6,7]:

$$\sum_{\vec{x}} \psi^\dagger(\vec{x}) \Gamma(\vec{x}) \chi^\dagger(\vec{x}), \quad (11)$$

using a gauge-invariant smearing function [22]

$$\Gamma(\vec{x}) \equiv \gamma^\dagger(\vec{x}) \Omega(\vec{x}) \gamma(\vec{x}), \quad (12)$$

where the  $2 \times 2$  spin matrix  $\Omega(\vec{x})$  selects the quantum numbers of interest, and

$$\gamma(x) = \left(1 + \epsilon \Delta^{(2)}(x)\right)^{n_s}. \quad (13)$$

The weight  $\epsilon$  and the number of smearing iterations  $n_s$  were adjusted to optimize the overlap with the ground state.

Meson correlation functions [6,7] were computed for the  $^1S_0$  ( $\Omega = I$ ),  $^3S_1$  ( $\Omega = \sigma_i$ ) and  $^1P_1$  ( $\Omega = \Delta_i$ ) mesons. The three triplet  $P$ -wave correlators ( $^3P_0$ ,  $^3P_1$ ,  $^3P_2$ ) were also analyzed, but this data is of insufficient quality to report here. Correlation functions were evaluated at both zero momentum and at the smallest allowed nonzero momentum.

## B. Simulation Parameters

Six lattices were generated using the mean link in Landau gauge to set the tadpole factor ( $u_{0,L}$ ) and seven lattices with comparable spacings were generated using average plaquette tadpoles ( $u_{0,P}$ ). The parameters of these thirteen lattices are given in Tables I and II. Note that we use  $\beta_L$  to denote the lattice coupling for simulations with  $u_{0,L}$ , and  $\beta_P$  for lattices with  $u_{0,P}$ . To check that finite volume effects are not an issue on the lattices with the smallest spacings, we performed some runs at  $\beta_P = 7.3$  on a  $16^4$  volume, and found no significant change in the results.

A standard Cabibbo-Marinari pseudo heat bath was used to generate the gauge field configurations. The number of updates between measurements varied from 10 for lattices with the largest spacings to 20 for the smallest; autocorrelation times satisfied  $\tau \lesssim 0.5$  in all cases. Smeared-smeared correlators were used, with typically 5–10 smearing iterations, and a smearing weight  $\epsilon = 1/12$  was used in all cases.

The lattice spacings were determined from the spin-averaged  $1P - 1S$  mass difference, which we set to 458 MeV (the experimental value for charmonium); this mass difference is thought to be about the same for all quarkonium systems [23]. The difference between the singlet  $^1P_1$  and the spin-averaged  $^3S_1$ ,  $^1S_0$  states was used for this purpose.

The bare quark masses were tuned by calculating the kinetic masses  $M_{\text{kin}}$  of the  $^1S_0$  states in physical units, which were extracted from fits to the energies  $E_{\mathbf{P}}$  of the boosted states using the form

$$E_{\mathbf{P}} - E_0 = \frac{\mathbf{P}^2}{2M_{\text{kin}}}. \quad (14)$$

Fits were made to the state with momentum components  $(1, 0, 0)$  in units of  $2\pi/(Na)$ ; relativistic corrections to the dispersion relation made little difference in the fit values of  $M_{\text{kin}}$ . The bare quark masses  $M_Q^0$  were fit to the following  $^1S_0$  kinetic masses:  $M_{c\bar{c}} = 2.98$  GeV,  $M_{b\bar{c}} = 6.28$  GeV, and  $M_{b\bar{b}} = 9.46$  GeV. The value of the  $b\bar{c}$   $S$ -wave meson mass adopted here was obtained in a previous NRQCD analysis of the  $b\bar{c}$  system [23].

A potential complication arises in that the lattice spacing and quark masses determined from different systems on the same quenched configurations do not generally agree. Since we compare results for a given system obtained over a wide range of lattice spacings, we have attempted to minimize systematic effects from tuning errors by re-tuning the parameters for each system on each ensemble of configurations. In the case of the  $b\bar{c}$  system we used the  $c$ -quark mass determined from the  $M_{c\bar{c}}$  kinetic mass, and tuned the  $b$ -quark mass to reproduce  $M_{b\bar{c}}$ . Note that the  $b$ -quark mass was re-tuned in simulations of the  $b\bar{b}$  system, to obtain the correct value of  $M_{b\bar{b}}$ . The final simulation results for the kinetic masses are accurate to within 3% in all cases.

The resulting quark masses and lattice spacings for the three quarkonium systems for the NRQCD action at  $O(v^6)$  are given in Tables III and IV. Note again that the lattice spacing is given separately for each system, the differences possibly reflecting effects due to quenching, which has been conjectured to play a role in setting the scale in these and other hadronic systems (see e.g. Ref. [23]). The  $b$ -quark mass is similarly given separately for the  $b\bar{c}$  and  $b\bar{b}$  systems. We found only small changes in the quark masses and lattice spacings when they are determined from the NRQCD action at  $O(v^4)$ .

Although we think that it is worthwhile to minimize systematic errors by re-tuning the quenched lattice parameters for the different quarkonium systems, and have done so in all simulations reported here, these effects are actually small. It is important to note that none of the conclusions reached in this study are changed if our re-tuning procedure is modified.

### III. RESULTS AND ANALYSIS

Hyperfine splittings for the three quarkonium systems  $c\bar{c}$ ,  $b\bar{c}$ , and  $b\bar{b}$  were extracted on the six lattices with  $u_{0,L}$  (cf. Table I), and the seven lattices with  $u_{0,P}$  (cf. Table II). To illustrate the quality of the raw data we show effective mass plots  $m_{\text{eff}}(T) = -\log(G(T)/G(T-1))$  for the  $b\bar{c}$  system at  $O(v^6)$ , on the two lattices with the smallest spacings, in Fig. 1 ( $\beta_L = 7.5$ ) and Fig. 2 ( $\beta_P = 7.3$ ).

Single exponential fits to the correlation functions were used to get the masses of the ground states, and a jackknife analysis was used to estimate statistical errors. The hyperfine splittings were obtained from a fit to the ratio of  $^3S_1$  and  $^1S_0$  correlation functions. Detailed fit results corresponding to the data in Figs. 1 and 2 are given in Tables V and VI. Final estimates of the dimensionless energies were obtained by finding two or three successive  $t_{\text{min}}/t_{\text{max}}$  intervals for which the fit results overlap within statistical errors. The largest statistical error in the overlapping fits was used as an estimate of the error in the final fit value. We give the final fit results for the dimensionless energies for the  $b\bar{c}$  states at  $O(v^6)$  in Tables VII and VIII.

The final fit results for all hyperfine splittings in physical units are given in Tables IX and X, where the quoted errors are purely statistical. We expect a systematic error of order 10% in the hyperfine splittings, coming from uncertainties in the quark mass determinations due to  $O(v^6)$  spin-independent relativistic corrections [7,17]. Effects due to quenching may also be large in the case of the charmonium hyperfine splitting [24], as the estimates from relativistic [24,10] and NRQCD [8] actions are all substantially smaller than the experimental value of  $(118 \pm 2)$  MeV.

The splittings for the  $c\bar{c}$ ,  $b\bar{c}$ , and the  $b\bar{b}$  systems are plotted against lattice spacing squared in Figs. 3, 4, and 5 respectively. For each system the splittings obtained with  $u_{0,L}$  and  $u_{0,P}$ , and at  $O(v^4)$  and  $O(v^6)$ , are plotted together in Figs. 3–5. We collect all results with  $u_{0,L}$  in Fig. 6, and all results with  $u_{0,P}$  in Fig. 7.

There are a number of very clear features in the data. To begin with, we note that the results with  $u_{0,L}$  for the three quarkonium systems show much smaller scaling violations than the results with  $u_{0,P}$  (compare Figs. 6 and 7). The smallest scaling violations are in the results with  $u_{0,L}$  at  $O(v^6)$ , which show remarkably little change as the lattice spacing is varied here by a factor of about 2.5. The  $b\bar{b}$  data show the largest scaling violations, as expected from the fact that this system should have the smallest size of the three. This scaling analysis provides evidence that  $u_{0,L}$  tadpole renormalization yields a more continuum-like action than does  $u_{0,P}$ . The improved scaling may also demonstrate indirectly that  $O(v^6)$  corrections improve the matching of NRQCD to true QCD, as expected.

Perhaps the most striking feature of the data is the sharp drop in the  $b\bar{c}$  splitting at smaller lattice spacings, when  $u_{0,P}$  is used at  $O(v^6)$  (see the filled circles in Fig. 4). In fact, most of the  $c$ -quark data with  $u_{0,P}$  show very large changes at the smallest lattice spacings. The  $u_{0,L}$  data on the other hand exhibit a much smoother behavior. Note for example that the  $O(v^6)$   $c\bar{c}$  splitting with  $u_{0,P}$  lies well below the data with  $u_{0,L}$ , except at the smallest lattice spacings, where the  $u_{0,P}$  data show a sharp upturn (compare the filled circles and filled squares in Fig. 3).

We interpret these features as possible indicators of a breakdown in the NRQCD effective action at smaller lattice spacings, when the bare quark mass in lattice units  $aM_Q^0$  falls below about one. From Tables III and IV we see that the bare  $c$ -quark mass for example turns out to be much larger when  $u_{0,L}$  is used, compared to when  $u_{0,P}$  is used on lattices with comparable spacings (compare  $aM_c^0 = 0.65$  at  $a_P \approx 0.14$  fm with  $aM_c^0 = 1.10$  at  $a_L \approx 0.16$  fm). Although there is clearly a pathological behavior in the  $c$ -quark simulations with  $u_{0,P}$  at smaller lattice spacings, we cannot reach definitive conclusions regarding the breakdown of the effective action without doing  $u_{0,L}$  simulations at much smaller  $aM_c^0$ . This requires lattices with much smaller spacings than we can realistically simulate.

Another key feature of these results is that the relativistic corrections to the hyperfine splittings are smaller when the action is renormalized using  $u_{0,L}$ , particularly for the  $c\bar{c}$  and  $b\bar{c}$  systems. We can make a rough estimate of the value of  $v^2$  from the change in the hyperfine splitting in going from  $O(v^4)$  to  $O(v^6)$ . For example, we find  $v_{c\bar{c}}^2 \approx 0.3\text{--}0.4$  when using  $u_{0,L}$ , compared to  $v_{c\bar{c}}^2 \approx 0.4\text{--}0.6$  when using  $u_{0,P}$ . Note that the  $u_{0,P}$  estimate of  $v^2$  depends very strongly on the lattice spacing, increasing rapidly as  $a$  decreases; this may be related to pathologies in the data at  $aM_c^0 \lesssim 1$ , discussed above.

The estimate of  $v_{c\bar{c}}^2$  obtained with  $u_{0,L}$  is consistent with naive estimates of operator expectation values in NRQCD [3]. Hence while the velocity expansion for charmonium is

subject to large corrections, it may not be as unreliable as was suggested in Ref. [8], based on simulations with  $u_{0,P}$  on fine lattices.

We note finally that it is reasonable to attempt to extrapolate the  $O(v^6)$  hyperfine splittings for  $c\bar{c}$  and  $b\bar{c}$  to zero lattice spacing, from the data on coarse lattices, where there is reasonably good scaling behavior (and where cutoff effects in the effective theory should be small, since  $aM_Q^0 > 1$  in this region [12]). However, the extrapolations in the  $u_{0,L}$  and  $u_{0,P}$  data, both of which exhibit good scaling on coarse lattices, are clearly very different (compare the filled circles with the filled squares in Fig. 3, and in Fig. 4). This suggests that some relevant operator coefficients  $c_i$  in the NRQCD action (Eqs. (8) and (9)) receive significant  $O(\alpha_s)$  corrections in one or both of the two tadpole schemes. This underlines the need to go beyond tree-level tadpole improvement in order to fully clarify the differences between renormalization schemes.

#### IV. SUMMARY

We have presented new evidence that clearly favors tadpole renormalization using the mean-link in Landau gauge over the fourth root of the average plaquette. This includes a demonstration of much better scaling behavior of the hyperfine splittings in three quarkonium systems when  $u_{0,L}$  is used, and a smaller size for spin-dependent relativistic corrections. The results presented here also help to elucidate the structure of the NRQCD effective action. In particular, we see signs of a breakdown in the NRQCD expansion when the bare quark mass falls below about one in lattice units, with pathological behavior clearly visible in the  $c$ -quark systems with  $u_{0,P}$  tadpoles. With  $u_{0,L}$  on the other hand the bare quark masses turn out to be much larger than with  $u_{0,P}$ , resulting in a much smoother behavior. We have in fact been unable to do realistic simulations on lattice fine enough to make  $aM_c^0 < 1$  with  $u_{0,L}$  tadpoles. At the same time, these results also serve to underline the need to go beyond tree-level matching of improved actions, in order to eliminate uncertainties due to uncalculated  $O(\alpha_s)$  renormalizations [18,19].

#### ACKNOWLEDGMENTS

We are indebted to C. T. H. Davies, G. P. Lepage, R. Lewis, and R. M. Woloshyn for many helpful discussions and suggestions. This work was supported in part by the Natural Sciences and Engineering Research Council of Canada.

## REFERENCES

- [1] G. P. Lepage and P. B. Mackenzie, Phys. Rev. D **48**, 2250 (1993).
- [2] G. P. Lepage and B. A. Thacker, Nucl. Phys. B (Proc. Suppl.) **4**, 199 (1988); B. A. Thacker and G. P. Lepage, Phys. Rev. D **43**, 196 (1991).
- [3] G. P. Lepage, L. Magnea, C. Nakhleh, U. Magnea and K. Hornbostel, Phys. Rev. D **46**, 4052 (1992).
- [4] C. T. H. Davies *et al.*, NRQCD Collaboration, Phys. Lett. B **345**, 42 (1995); Phys. Rev. D **56**, 2755 (1997).
- [5] C. T. H. Davies *et al.*, NRQCD Collaboration, Phys. Rev. Lett. **73**, 2654 (1994).
- [6] C. T. H. Davies *et al.*, NRQCD Collaboration, Phys. Rev. D **50**, 6963 (1994).
- [7] C. T. H. Davies *et al.*, NRQCD Collaboration, Phys. Rev. D **52**, 6519 (1995).
- [8] H. D. Trottier, Phys. Rev. D **55**, 6844 (1997).
- [9] M. G. Alford, T. R. Klassen and G. P. Lepage, unpublished. See also G. P. Lepage, Nucl. Phys. A (Proc. Suppl.) **60**, 267 (1998).
- [10] M. G. Alford, T. R. Klassen and G. P. Lepage, Report No. hep-lat/9712005.
- [11] N. H. Shakespeare and H. D. Trottier, in preparation; N. H. Shakespeare, M.Sc. thesis, Simon Fraser University (1996).
- [12] C. T. H. Davies *et al.*, NRQCD Collaboration, Report No. hep-lat/9802024. See also C. T. H. Davies, Nucl. Phys. A (Proc. Suppl.) **60**, 124 (1998);
- [13] T. Manke, I. T. Drummond, R. R. Horgan, and H. P. Shanahan, Phys. Lett. B **408**, 308 (1997).
- [14] A. Spitz *et al.*, SESAM Collaboration, Report No. hep-lat/9709138
- [15] A. Ali Khan and T. Bhattacharya, Nucl. Phys. B (Proc. Suppl.) **53**, 368 (1997)
- [16] K.-I. Ishikawa *et al.*, Phys. Rev. D **56**, 7028 (1997).
- [17] R. Lewis and R. M. Woloshyn, in preparation.
- [18] Work on nonperturbative matching of lattice actions has been reported in M. Lüscher *et al.*, Nucl. Phys. B **491**, 323 (1997), and references therein.
- [19] Some preliminary work on perturbative matching of spin-dependent operators in NRQCD and clover-fermion actions has been reported in H. D. Trottier and G. P. Lepage, Report No. hep-lat/9710015.
- [20] See for example C. T. H. Davies *et al.*, Phys. Rev. D **37**, 1581 (1988).
- [21] M. Alford, W. Dimm, G. P. Lepage, G. Hockney, and P. B. Mackenzie, Phys. Lett. **B361**, 87 (1995).
- [22] The smearing function  $\Gamma(\vec{x})$  used here is identical to the one used in Ref. [8]. Note that Eq. (22) for  $\Gamma(\vec{x})$  in Ref. [8] is incorrect, and should read as given here in Eq. (12).
- [23] C. T. H. Davies *et al.*, NRQCD Collaboration, Phys. Lett. **B382**, 131 (1996); C. T. H. Davies *et al.*, UKQCD Collaboration, Report No. hep-lat/9710069.
- [24] A. El-Khadra and B. Mertens, Nucl. Phys. B (Proc. Suppl.) **42**, 406 (1995); A. El-Khadra, Nucl. Phys. B (Proc. Suppl.) **26**, 372 (1992). More recent results are reviewed in J. Shigemitsu, Nucl. Phys. B (Proc. Suppl.) **53**, 16 (1997).

## TABLES

$\beta_L$	$\langle \frac{1}{3} \text{ReTr} U_\mu \rangle$	$\langle \frac{1}{3} \text{ReTr} U_{\text{pl}} \rangle^{1/4}$	$a_{c\bar{c}}$ (fm)	Volume
7.5	0.836	0.879	0.16	$12^3 \times 16$
7.4	0.829	0.875	0.18	$10^3 \times 16$
7.0	0.780	0.850	0.28	$6^3 \times 10$
6.85	0.763	0.840	0.32	$6^3 \times 10$
6.7	0.750	0.830	0.36	$6^3 \times 10$
6.6	0.743	0.825	0.38	$6^3 \times 10$

TABLE I. Simulation parameters using the Landau gauge mean-link to determine the tadpole renormalization  $u_{0,L}$  (second column). The lattice spacing determined from the charmonium system is given as a guide.

$\beta_P$	$\langle \frac{1}{3} \text{ReTr} U_\mu \rangle$	$\langle \frac{1}{3} \text{ReTr} U_{\text{pl}} \rangle^{1/4}$	$a_{c\bar{c}}$ (fm)	Volume
7.3	0.837	0.878	0.14	$12^3 \times 16$
7.2	0.830	0.875	0.17	$10^3 \times 16$
7.0	0.812	0.864	0.21	$8^3 \times 10$
6.8	0.791	0.854	0.26	$6^3 \times 10$
6.6	0.771	0.841	0.31	$6^3 \times 10$
6.4	0.753	0.829	0.35	$6^3 \times 10$
6.25	0.741	0.821	0.39	$6^3 \times 10$

TABLE II. Simulation parameters using the average plaquette to determine the tadpole renormalization  $u_{0,P}$  (third column).

$\beta_L$	$c\bar{c}$		$b\bar{c}$		$b\bar{b}$	
	$a$ (fm)	$aM_c^0[n]$	$a$ (fm)	$aM_b^0[n]$	$a$ (fm)	$aM_b^0[n]$
7.5	0.155(4)	1.10[4]	0.138(4)	3.20[2]	0.128(3)	3.20[2]
7.4	0.179(2)	1.20[4]	0.161(2)	3.57[2]	0.152(2)	3.57[2]
7.0	0.280(4)	1.97[2]	0.261(4)	6.10[2]	0.257(3)	5.35[2]
6.85	0.319(5)	2.25[2]	0.299(5)	6.50[2]	0.296(4)	5.90[2]
6.7	0.361(6)	2.50[2]	0.339(6)	7.20[2]	0.343(6)	6.35[2]
6.6	0.380(7)	2.67[2]	0.363(7)	7.50[2]	0.363(7)	6.66[2]

TABLE III. Lattice spacings and bare quark masses for the three quarkonium systems at  $O(v^6)$ , using Landau gauge mean-link tadpoles  $u_{0,L}$ ; the stability parameter  $n$  for each mass is given in square brackets.

$\beta_P$	$c\bar{c}$		$b\bar{c}$		$b\bar{b}$	
	$a$ (fm)	$aM_c^0[n]$	$a$ (fm)	$aM_b^0[n]$	$a$ (fm)	$aM_b^0[n]$
7.3	0.140(4)	0.65[8]	0.131(4)	2.87[2]	0.127(4)	2.87[2]
7.2	0.169(2)	0.83[4]	0.150(2)	3.20[2]	0.145(2)	3.20[2]
7.0	0.210(2)	1.10[4]	0.191(2)	4.10[2]	0.185(2)	3.95[2]
6.8	0.256(3)	1.43[3]	0.235(3)	4.98[2]	0.228(3)	4.53[2]
6.6	0.313(4)	1.80[3]	0.288(4)	5.83[2]	0.284(4)	5.23[2]
6.4	0.350(6)	2.15[2]	0.328(6)	6.45[2]	0.328(6)	5.60[2]
6.25	0.390(6)	2.41[2]	0.363(7)	6.85[2]	0.362(6)	5.99[2]

TABLE IV. Lattice spacings and bare quark masses for the three quarkonium systems at  $O(v^6)$  using average plauquette tadpoles  $u_{0,P}$ .

$t_{\min}/t_{\max}$	$^1P_1$	$^3S_1$	$^1S_0$	$^3S_1 - ^1S_0$
2/16	0.627(9)	0.306(2)	0.285(1)	0.0210(3)
3/16	0.621(10)	0.305(2)	0.284(1)	0.0212(3)
4/16	0.618(12)	0.305(2)	0.284(1)	0.0212(4)
5/16	0.615(14)	0.305(2)	0.284(2)	0.0210(4)
6/16	0.612(17)	0.304(2)	0.283(2)	0.0209(4)
7/16	0.606(20)	0.304(2)	0.283(2)	0.0207(5)
8/16	0.598(24)	0.303(2)	0.283(2)	0.0205(5)
9/16	0.586(30)	0.303(2)	0.283(2)	0.0205(6)
10/16	0.591(39)	0.304(2)	0.283(2)	0.0204(7)

TABLE V. Examples of fits to the  $O(v^6)$   $b\bar{c}$  spectra at  $\beta_L = 7.5$  ( $a \approx .14$  fm).

$t_{\min}/t_{\max}$	$^1P_1$	$^3S_1$	$^1S_0$	$^3S_1 - ^1S_0$
2/16	0.879(9)	0.578(2)	0.581(2)	-0.0029(3)
3/16	0.874(10)	0.577(2)	0.579(2)	-0.0028(3)
4/16	0.872(12)	0.577(2)	0.579(2)	-0.0027(3)
5/16	0.870(14)	0.577(2)	0.580(2)	-0.0026(4)
6/16	0.871(17)	0.577(2)	0.580(2)	-0.0026(4)
7/16	0.877(21)	0.579(2)	0.581(2)	-0.0026(5)
8/16	0.885(25)	0.579(2)	0.582(2)	-0.0027(5)

TABLE VI. Examples of fits to the  $O(v^6)$   $b\bar{c}$  spectra at  $\beta_P = 7.3$  ( $a \approx .13$  fm).

$\beta_L$	$^1P_1$	$^3S_1$	$^1S_0$	$^3S_1 - ^1S_0$
7.5	0.62(1)	0.305(2)	0.284(1)	0.0212(3)
7.4	0.70(1)	0.330(1)	0.306(1)	0.0235(2)
7.0	0.95(1)	0.346(1)	0.310(1)	0.0356(3)
6.85	1.01(1)	0.329(1)	0.287(1)	0.0425(3)
6.7	1.08(2)	0.308(1)	0.261(1)	0.0460(4)
6.6	1.12(2)	0.292(1)	0.245(1)	0.0471(3)

TABLE VII. Final fit results for the dimensionless energies for the  $O(v^6)$   $b\bar{c}$  spectra using  $u_{0,L}$ .

$\beta_P$	$^1P_1$	$^3S_1$	$^1S_0$	$^3S_1 - ^1S_0$
7.3	0.87(1)	0.577(2)	0.580(2)	-0.0027(3)
7.2	0.98(1)	0.637(1)	0.629(1)	0.0074(1)
7.0	1.12(1)	0.681(1)	0.666(1)	0.0138(1)
6.8	1.25(1)	0.706(1)	0.687(1)	0.0189(2)
6.6	1.36(1)	0.699(1)	0.676(1)	0.0233(2)
6.4	1.44(2)	0.681(1)	0.654(1)	0.0263(2)
6.25	1.48(2)	0.648(1)	0.621(1)	0.0277(2)

TABLE VIII. Final fit results for the dimensionless energies for the  $O(v^6)$   $b\bar{c}$  spectra using  $u_{0,P}$ .

$\beta_L$	$O(v^6)$			$O(v^4)$		
	$c\bar{c}$	$b\bar{c}$	$b\bar{b}$	$c\bar{c}$	$b\bar{c}$	$b\bar{b}$
7.5	56.0(24)	30.2(14)	28.9(12)			
7.4	53.8(9)	28.7(5)	26.8(4)	84.5(15)	47.0(9)	31.9(5)
7.0	52.0(11)	26.8(6)	23.2(5)	76.9(17)	38.3(9)	25.0(5)
6.85	52.4(12)	28.0(7)	22.0(5)			
6.7	50.1(12)	26.8(7)	20.3(5)			
6.6	48.9(11)	25.6(6)	19.2(5)	69.8(17)	34.0(9)	21.5(5)

TABLE IX. Final fit results for hyperfine splittings in MeV for the three quarkonium systems, with  $u_{0,L}$  tadpole renormalization.

$\beta_P$	$O(v^6)$			$O(v^4)$		
	$c\bar{c}$	$b\bar{c}$	$b\bar{b}$	$c\bar{c}$	$b\bar{c}$	$b\bar{b}$
7.3	76.4(36)	-4.2(3)	22.7(10)			
7.2	39.8(7)	9.7(2)	21.5(4)	100.4(18)	45.2(8)	26.3(4)
7.0	34.9(6)	14.2(3)	19.2(4)			
6.8	33.0(7)	15.8(3)	17.1(3)	72.8(15)	32.1(7)	19.4(4)
6.6	30.7(6)	16.0(4)	14.6(3)			
6.4	29.3(7)	15.8(4)	13.3(3)			
6.25	27.7(6)	15.1(4)	12.2(3)	46.8(11)	22.3(6)	13.8(3)

TABLE X. Final fit results for hyperfine splittings in MeV for the three quarkonium systems, with  $u_{0,P}$  tadpole renormalization.

## FIGURES

FIG. 1. Effective mass plot for  $O(v^6)$   $b\bar{c}$  spectra at  $\beta_L = 7.5$  ( $a \approx 0.14$  fm): (a)  $^1P_1$  state ( $\square$ ) and  $^1S_0$  state ( $\circ$ ); (b) hyperfine splitting.

FIG. 2. Effective mass plot for  $O(v^6)$   $b\bar{c}$  spectra at  $\beta_P = 7.3$  ( $a \approx 0.13$  fm): (a)  $^1P_1$  state ( $\square$ ) and  $^1S_0$  state ( $\circ$ ); (b) hyperfine splitting.

FIG. 3. Hyperfine splittings for the  $c\bar{c}$  system versus lattice spacing squared.

FIG. 4. Hyperfine splittings for the  $b\bar{c}$  system versus lattice spacing squared.

FIG. 5. Hyperfine splittings for the  $b\bar{b}$  system versus lattice spacing squared.

FIG. 6. Hyperfine splittings with  $u_{0,L}$  versus lattice spacing squared.

FIG. 7. Hyperfine splittings with  $u_{0,P}$  versus lattice spacing squared.

Figure 1a  
 $\beta_L = 7.5$

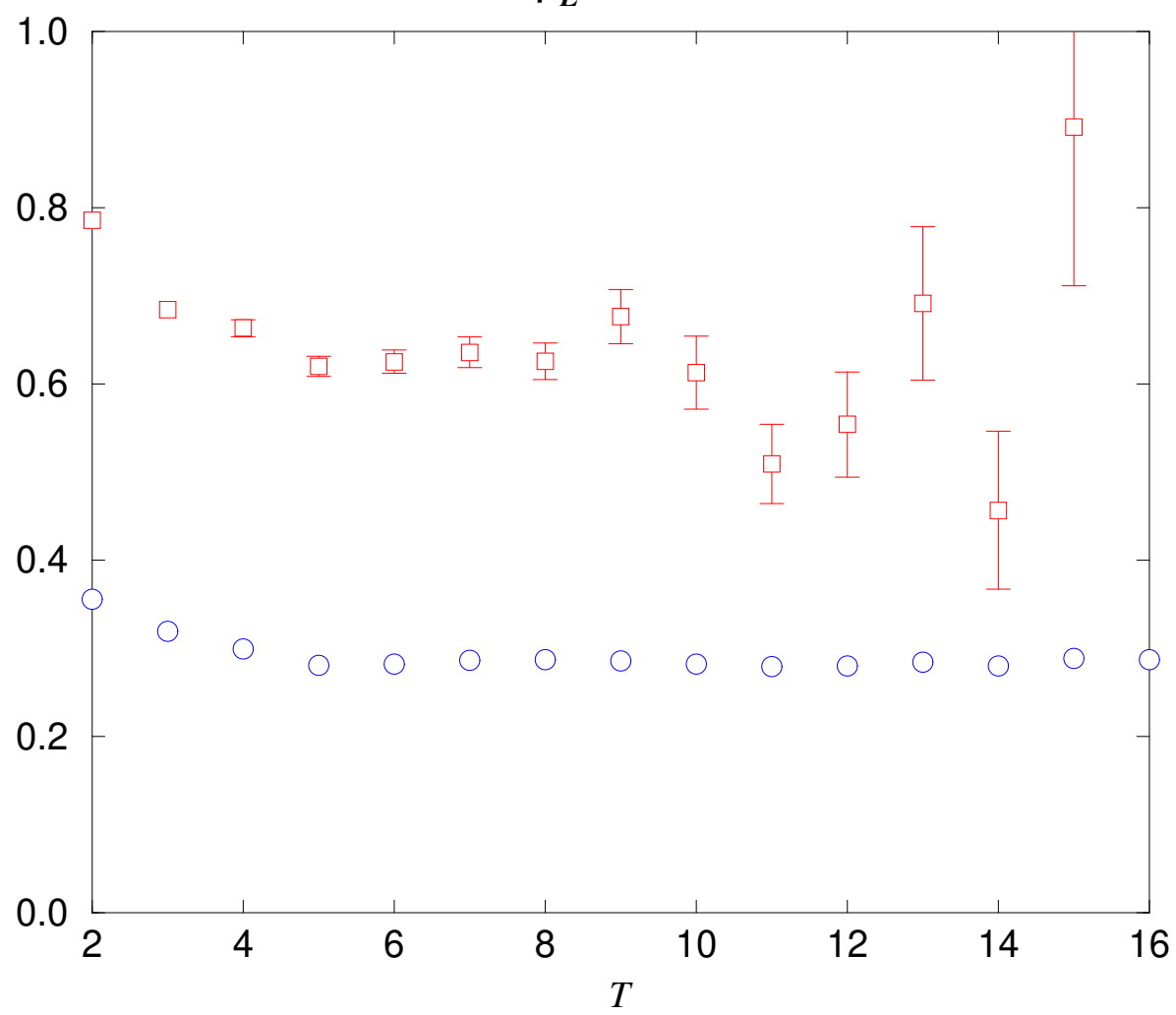


Figure 1b  
 $\beta_L = 7.5$

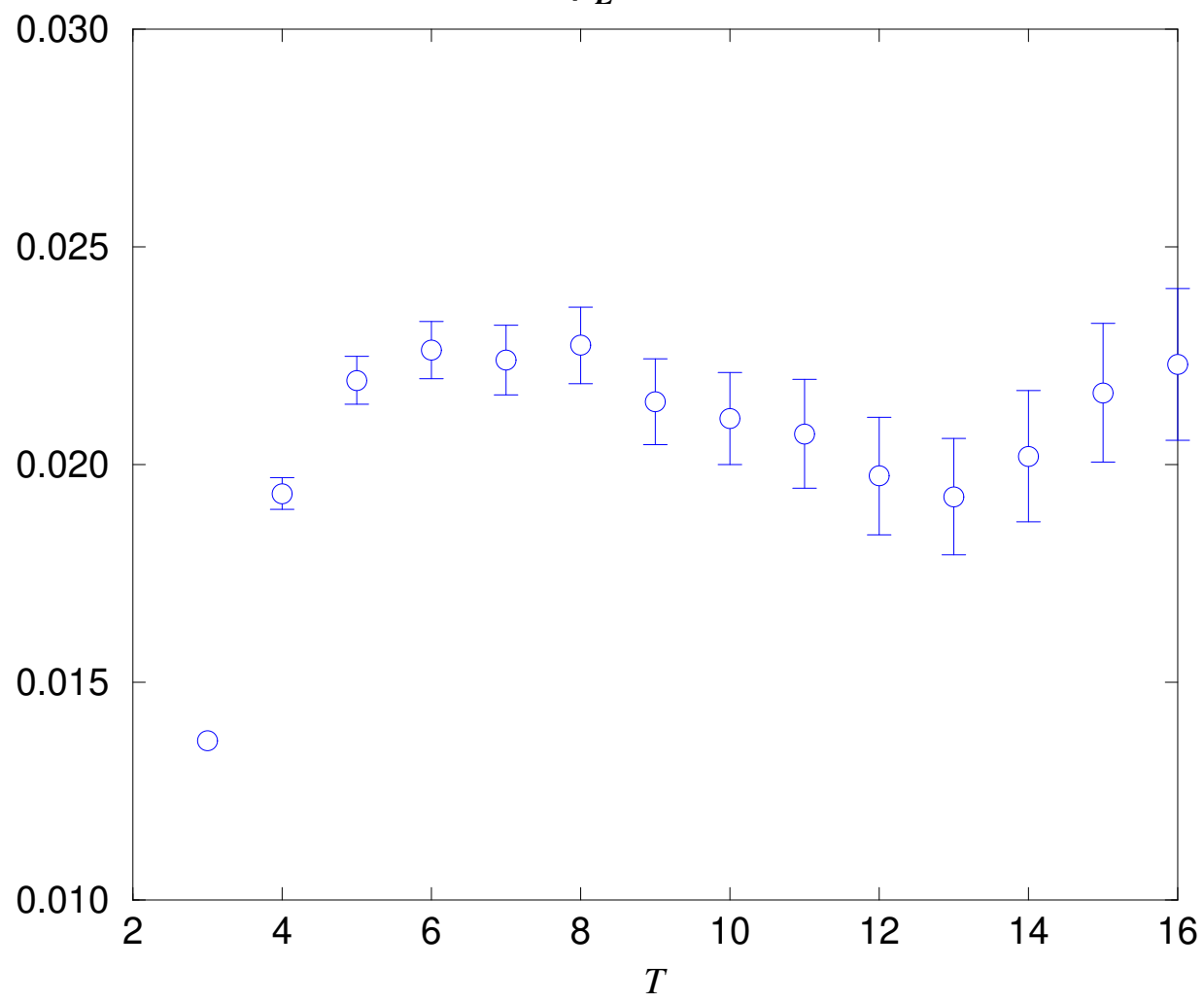


Figure 2a

$$\beta_p = 7.3$$

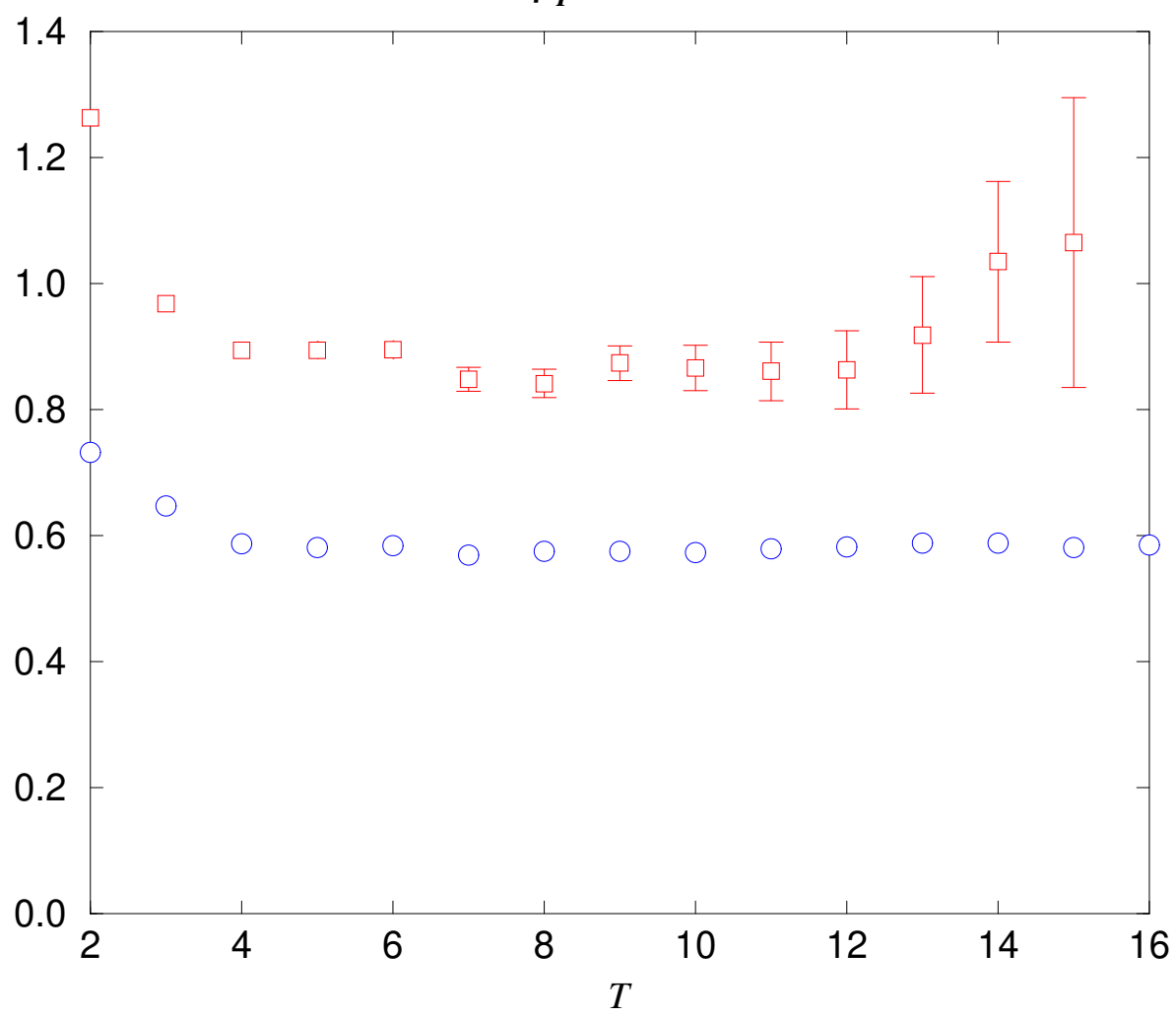


Figure 2b

$$\beta_p = 7.3$$

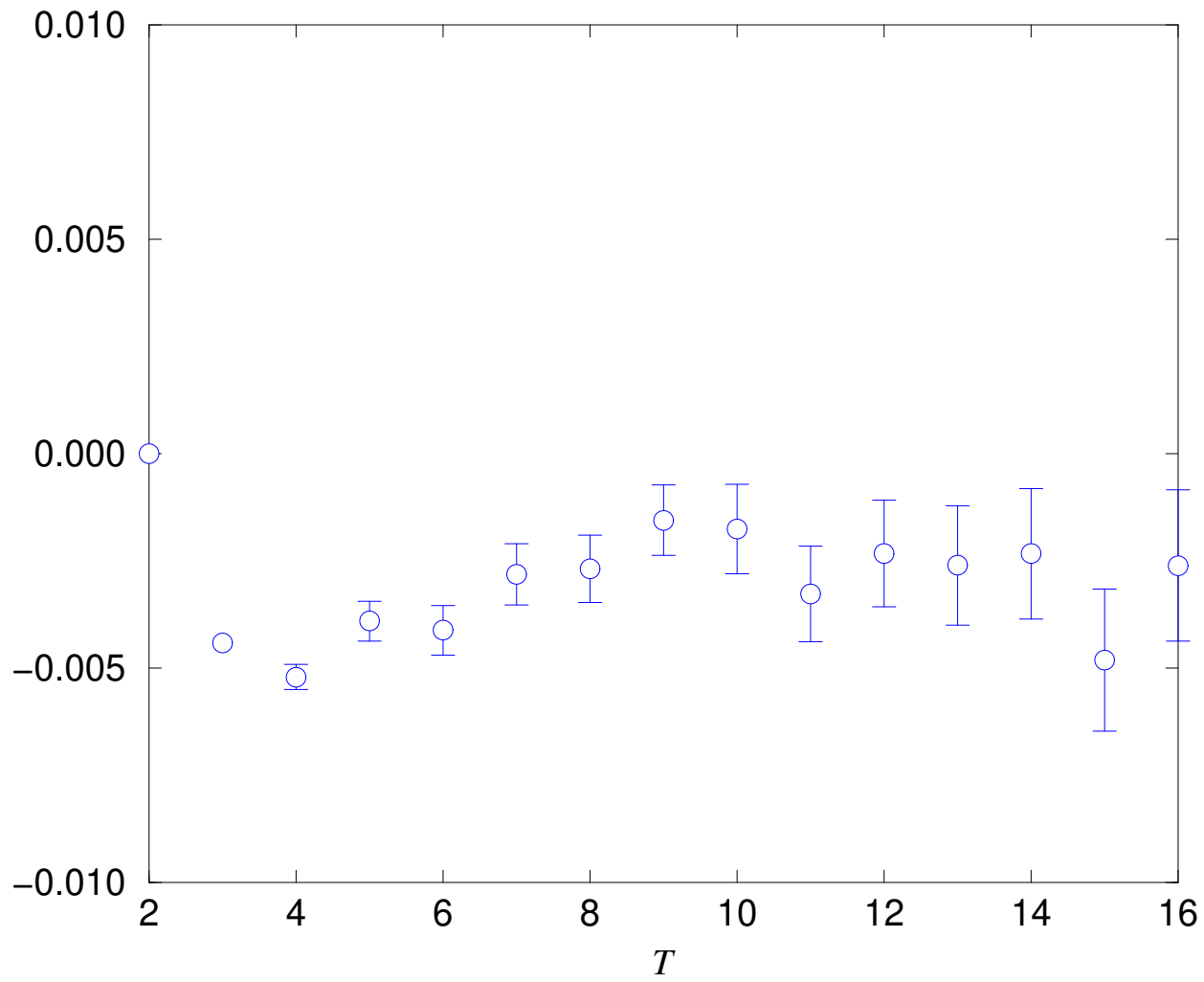


Figure 3  
 $c\bar{c}$

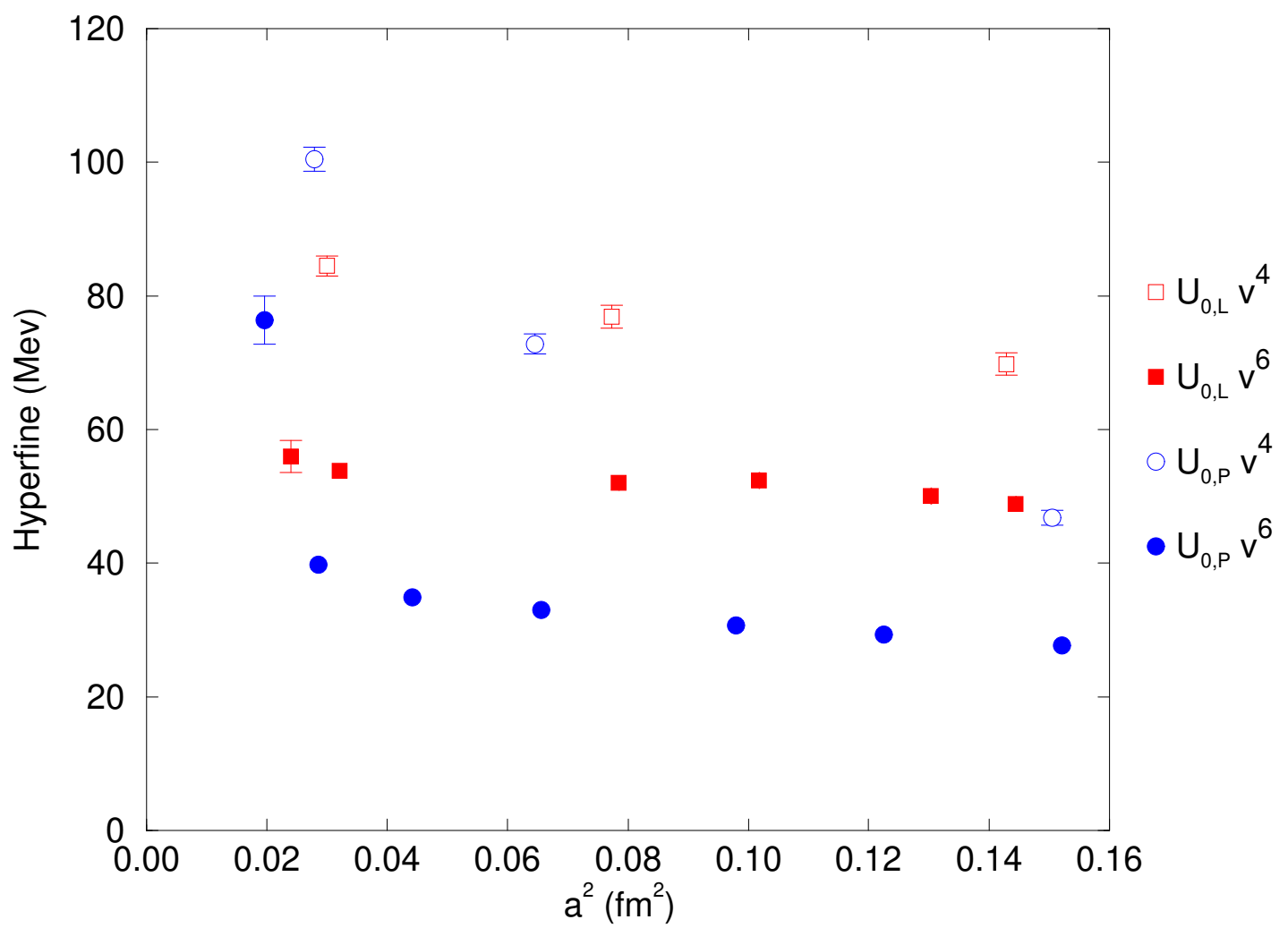


Figure 4  
 $b\bar{c}$

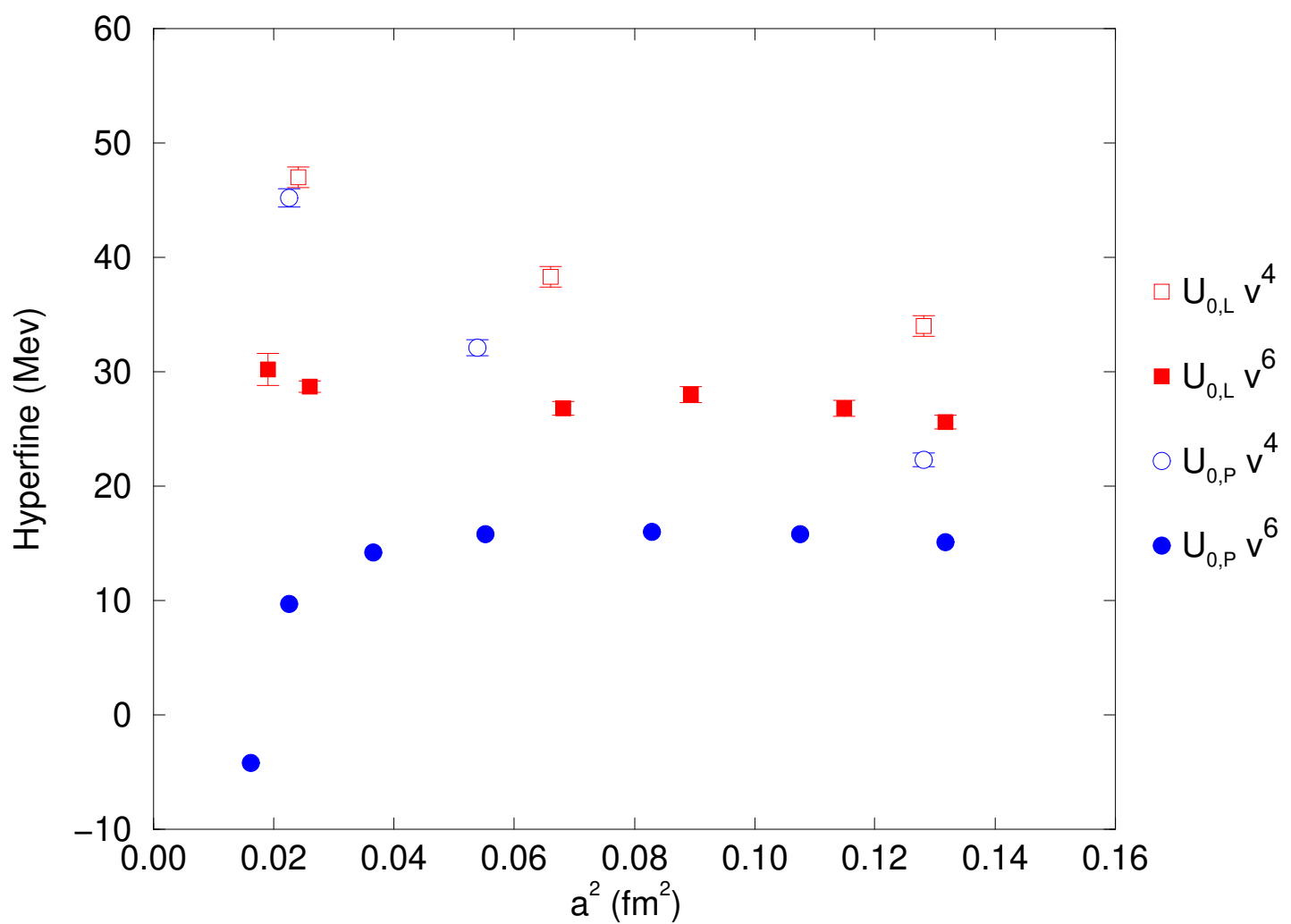


Figure 5  
 $b\bar{b}$

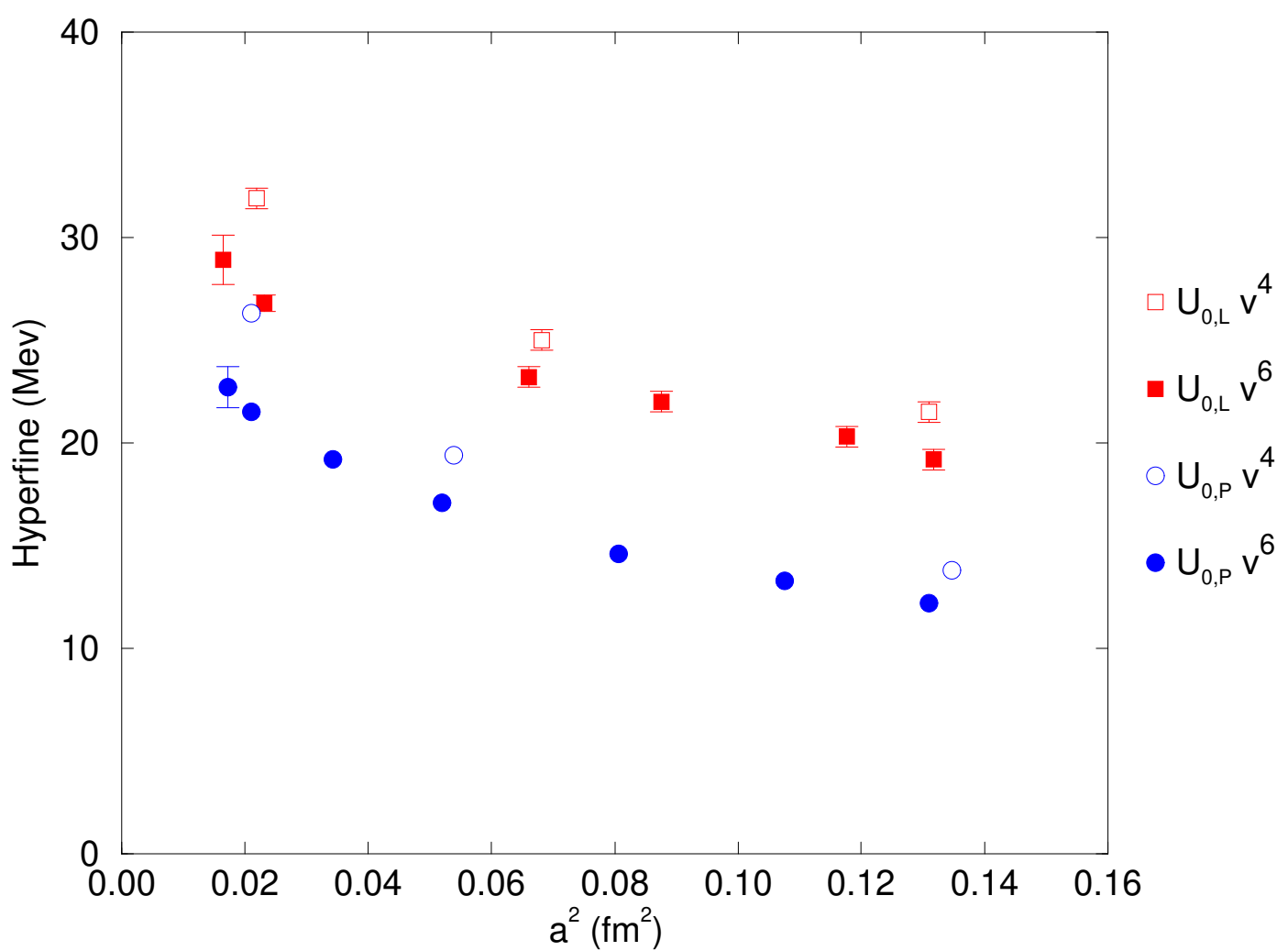


Figure 6  
 $U_{0,L}$

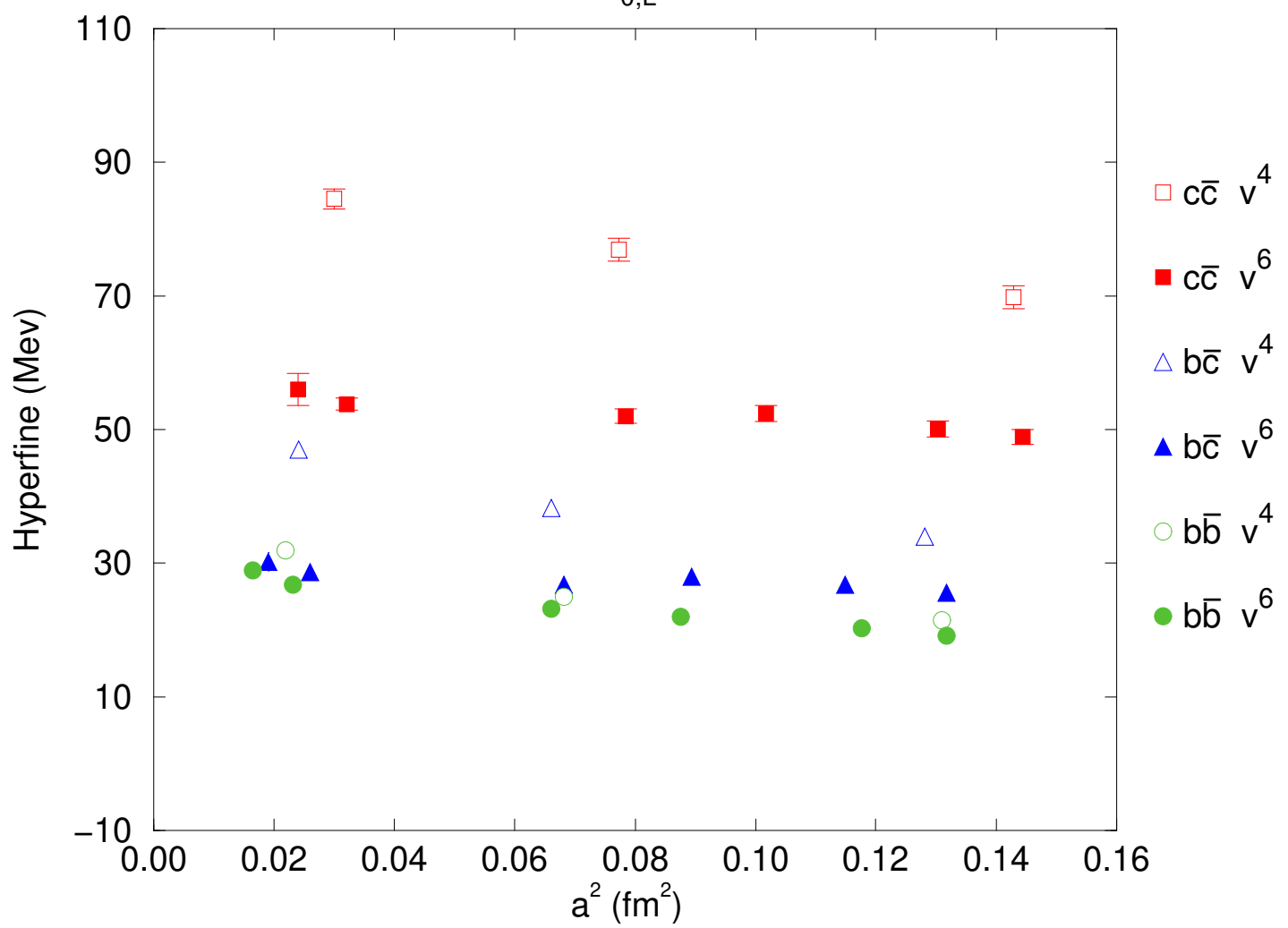


Figure 7  
 $U_{0,P}$

